MCB
Journals.ASM.org

Distinct Phospholipase C-β Isozymes Mediate Lysophosphatidic Acid Receptor 1 Effects on Intestinal Epithelial Homeostasis and Wound Closure

Sei-Jung Lee,[a] Giovanna Leoni,[b] Philipp-Alexander Neumann,[b] Jerold Chun,[c] Asma Nusrat,[b] C. Chris Yun[a,d]

Division of Digestive Diseases, Department of Medicine, Emory University School of Medicine, Atlanta, Georgia, USA[a]; Department of Pathology and Laboratory Medicine, Emory Epithelial Pathobiology and Mucosal Inflammation Research Unit, Emory University School of Medicine, Atlanta, Georgia, USA[b]; Department of Molecular Biology, The Scripps Research Institute, La Jolla, California, USA[c]; Winship Cancer Institute, Emory University School of Medicine, Atlanta, Georgia, USA[d]

Maintenance of the epithelial barrier in the intestinal tract is necessary to protect the host from the hostile luminal environment. Phospholipase C-β (PLC-β) has been implicated to control myriad signaling cascades. However, the biological effects of selective PLC-β isozymes are poorly understood. We describe novel findings that lysophosphatidic acid (LPA) regulates PLC-β1 and PLC-β2 via two distinct pathways to enhance intestinal epithelial cell (IEC) proliferation and migration that facilitate wound closure and recovery of the intestinal epithelial barrier. LPA acting on the LPA_1 receptor promotes IEC migration by facilitating the interaction of Gαq with PLC-β2. LPA-induced cell proliferation is PLC-β1 dependent and involves translocation of Gαq to the nucleus, where it interacts with PLC-β1 to induce cell cycle progression. An *in vivo* study using LPA_1-deficient mice (*Lpar1*$^{-/-}$) shows a decreased number of proliferating IECs and migration along the crypt-luminal axis. Additionally, LPA enhances migration and proliferation of IECs in an LPA_1-dependent manner, and *Lpar1*$^{-/-}$ mice display defective mucosal wound repair that requires cell proliferation and migration. These findings delineate novel LPA_1-dependent lipid signaling that facilitates mucosal wound repair via spatial targeting of distinct PLC-βs within the cell.

The intestinal tract is lined primarily with columnar epithelial cells that are regenerated every 4 to 5 days in rodents (1). The rapid turnover of the intestinal epithelium is maintained by stem cells residing at the crypt base. Turnover of the intestinal epithelium involves a series of actions that include proliferation at the crypt base, migration and differentiation along the crypt-luminal axis, and ultimately, regulated shedding at the luminal surface (1). The epithelial lining covering the gastrointestinal tract protects the host against threats that constantly arise from the external world. In response to injury, epithelial cells at the wound edge proliferate and migrate to cover denuded surfaces and reestablish the critical barrier function. Thus, rapid resealing of epithelial wounds is critical in maintaining intestinal mucosal homeostasis and in protecting the host from a hostile luminal environment.

Lysophosphatidic acid (LPA) is one of the smallest glycerophospholipids that elicits diverse biological effects, including cell migration and proliferation (2, 3). LPA has been reported to ameliorate epithelial damage in chemical-induced colitis in rats (4). However, the underlying cellular mechanisms and its receptor specificity involved in this process remain largely unknown. LPA produces a variety of cellular responses through its cognate receptors that include at least 6 members of the G protein-coupled LPA receptors (GPCRs), LPA_1 to LPA_6 (2, 3). LPA receptors are coupled to at least three heterotrimeric G proteins, Gαi/o, Gαq/11, and Gα12/13, and multiple LPA receptors are expressed in intestinal epithelial cells (IECs) (5). LPA receptors are expressed in the intestinal epithelial cells in the following order: $LPA_1 > LPA_5 \gg LPA_2$, LPA_3, LPA_4 (5). LPA_2 stimulates proliferation and migration of colon cancer cells, and the absence of LPA_2 suppresses the progression of colon cancer (6, 7). LPA_2 and LPA_5 are important for regulation of electrolytes and fluid transport in the intestine (5, 8). Despite being the most abundant LPA receptor in the small intestine and colon (5, 9), the importance of LPA_1 in the intestinal tract under physiological or pathological conditions remains elusive.

The phospholipase β (PLC-β) family consists of four members, PLC-β1 to -β4, that share the same primary structure and regulatory mode. PLC hydrolyzes phosphatidylinositol 4,5-biphosphate to generate inositol 1,4,5-triphosphate and diacylglycerol (10). Emerging evidence points to subtype-specific roles of PLC-β isozymes. However, why multiple forms of PLC-β are expressed in the same cell and how cells selectively regulate different PLC-β isozymes are not well understood. In this study, we present novel findings that LPA_1 regulates distinct PLC-β isozymes to enhance proliferation and migration of IECs. PLC-β1 and PLC-β2 are spatially targeted to the different cellular locations to achieve divergent outcomes. *In vivo* studies show defective mucosal wound repair arising from altered IEC proliferation and migration in the absence of LPA_1. These findings elucidate a novel role of LPA_1 in wound repair and provide a functional linkage between lipid signaling and intestinal epithelial homeostasis.

MATERIALS AND METHODS

Chemicals and antibodies. LPA (18:1; 1-oleoyl-2-hydroxy-*sn*-glycero-3-phosphate) was purchased from Avanti Polar Lipids (Alabaster, AL) and

Received 9 January 2013 Returned for modification 11 February 2013
Accepted 5 March 2013
Published ahead of print 11 March 2013
Address correspondence to C. Chris Yun, ccyun@emory.edu.
Supplemental material for this article may be found at http://dx.doi.org/10.1128/MCB.00038-13.

doi:10.1128/MCB.00038-13

prepared according to the manufacturer's instructions. For *in vitro* study, LPA was used at the final concentration of 1 μM in phosphate-buffered saline (PBS) containing 0.1% bovine serum albumin (BSA) unless otherwise specified. An equal volume of PBS containing 0.1% BSA was added as a control. Ki16425 was used at the final concentration of 10 μM for *in vitro* study as described previously (11, 12). When needed, pertussis toxin (PTX; 100 mg/ml), U73122 (5 μM), NSC23766 (10 μM), Y27632 (50 μM), or CK869 (10 μM) was used, and an equal volume of dimethyl sulfoxide (DMSO) was added as a vehicle control in all experiments. Mouse anti-vesicular stomatitis virus glycoprotein (anti-VSVG) P5D4 antibody was described previously (13). The following antibodies were purchased: rabbit anti-Ki67 antibody (Leica Microsystems, Buffalo Grove, IL); rabbit anti-LPA_1 antibody (Cayman Chemical, Ann Arbor, MI); mouse anti-Rac1 and mouse anti-Gαq antibodies (BD Biosciences, Franklin Lakes, NJ); mouse anti-Flag, mouse antihemagglutinin (anti-HA), and mouse anti-actin antibodies (Sigma-Aldrich, St. Louis, MO); rabbit anti-RhoA, rabbit anti-PLC-β1, rabbit anti-PLC-β2, and rabbit anti-PLC-β3 antibodies (Santa Cruz Biotechnology, Paso Robles, CA); and rabbit anti-Gα13, rabbit anti-Gαi, rabbit anti-cyclin D1, and mouse anti-Cdk4 (Cell Signaling Technology, Danvers, MA).

Cell culture and plasmids. Young adult mouse colon (YAMC) cells and mouse small intestine epithelium (MSIE) that harbor a heat-labile SV40 large T antigen expressed under the control of a gamma interferon (IFN-γ)-inducible promoter were the kind gift of Robert H. Whitehead (Vanderbilt University Medical Center) (14). The cells are grown in RPMI 1640 medium containing 5% fetal bovine serum (FBS), 50 U/ml penicillin, 50 μg/ml streptomycin, and 1% ITS Premix (6.25 mg/liter insulin, 6.25 mg/liter transferrin, 6.25 μg/liter selenous acid, 1.25 g/liter bovine serum albumin, and 5.35 mg/liter linoleic acid) under permissive conditions at 33°C in a humidified atmosphere with 5% CO_2 until confluent. Before all experiments, cells were cultured in IFN-γ-free medium under nonpermissive conditions of 37°C for 24 h. Rat intestinal epithelial cells (IEC-6) obtained from the American Tissue Culture Collection were grown in Dulbecco's modified Eagle medium (DMEM) supplemented with 5% FBS, 50 U/ml penicillin, 50 μg/ml streptomycin, and 4 μg/ml insulin at 37°C in a 95% air, 5% CO_2 atmosphere. All the cells were serum starved 24 h before LPA treatment in their appropriate medium without FBS. The pcDNA3.1 plasmids harboring HA-Rac1, HA-Rac1G12V (constitutively active form), HA-Rac1T17N (dominant negative), Glu-Glu-tagged Gαq (EE-Gαq), EE-Gα13, or EE-Gαi were obtained from the Missouri S&T cDNA Resource Center (Rolla, MO). PLC-β clones were gifts from Pann-Ghill Suh (Ulsan National Institute of Science and Technology, Republic of Korea). Transient transfection was performed using Lipofectamine 2000 (Invitrogen, Grand Island, NY). Stable expression of LPA_1 and LPA_2 was achieved by transduction with lentiviral pCDH/VSVG-LPA_1 and pCDH/VSVG-LPA_2, respectively. Lentiviral pCDH was used as a control. pLKO.1 plasmid harboring shLPA_1, shLPA_2, shPLC-β1, or shPLC-β2 was obtained from Sigma. pLKO.1-puro was used to generate control lentivirus, shCont. Specified cells transfected with lentivirus were selected by 10 μg/ml puromycin to obtain stably transfected cells. Silencing of gene products was confirmed by reverse transcription-PCR (RT-PCR) or Western blot.

Gα carboxyl-terminal minigenes. The cDNA minigene constructs were designed as encoding the last 11 amino acids of Gα subunits, Gαq and Gα13 (15), and the constructs were ligated into pcDNA3.1 plasmids (Invitrogen). The expression of minigenes in transfected cells was confirmed by RT-PCR (5). The following primer pairs corresponding to the Gα carboxyl-terminal sequence were used to verify the presence of the insert in cells: 5′-ATCCGCCGCCACCATGGGA-3′ and 5′-GCGAAAGGAGCGGGCGCTA-3′. These primers amplify a 434-bp fragment only if the Gα insert is present.

Animals. Founder BALB/c mice heterozygous for the LPA_1 receptor allele (*Lpar1*$^{+/-}$) were previously developed (16). *Lpar1*$^{+/-}$ mice were crossbred to generate *Lpar1*$^{+/+}$ (wild type [WT]), *Lpar1*$^{+/-}$, and *Lpar1*$^{-/-}$ littermates, which were used in all studies. All data represent results of at least two independent series of experiments. Experiments with animals were carried out under approval by the Institutional Animal Care and Use Committee of Emory University and in accordance with the NIH Guide for the Care and Use of Laboratory Animals.

Measurement of cell migration, proliferation, and apoptosis. To determine IEC migration, 8-week-old *Lpar1*$^{-/-}$ and WT littermates were given 5-bromo-2′-deoxyuridine (BrdU; 50 mg/kg of body weight) by intraperitoneal (i.p.) injection. At 2, 24, and 48 h after the injection, mice (8 mice per time point per group) were sacrificed and small intestine and colon were removed, flushed with ice-cold PBS, cut longitudinally, and formed into Swiss rolls. Tissue samples were fixed in 10% buffered formalin overnight, embedded in paraffin blocks, and cut into 0.4-μm sections for histological analysis. Paraffin-embedded sections were deparaffinized, labeled with rat anti-BrdU antibody, and finally subjected to either immunohistochemical or immunofluorescence staining as described previously (6, 17). The extent of cell migration was determined in a blinded manner by measuring the distance between the crypt base and the highest labeled cell along the crypt-villus axis. Other samples were subjected to hematoxylin and eosin (H&E) for histological examination. To determine IEC proliferation, mice were given 5-ethynyl-2′-deoxyuridine (EdU; 100 mg/kg) by i.p. injection and sacrificed after 1 h. Intestinal and colonic sections were prepared as described above. EdU incorporation into DNA was detected using the Click-iT EdU Alexa Fluor imaging kit (Invitrogen). The apoptotic cells in paraffin-embedded sections were detected by a terminal deoxynucleotidyl transferase dUTP nick end labeling (TUNEL) assay using an apoptosis detection kit (R&D Systems, Minneapolis, MN). All images were taken using a Zeiss Axioskop2 Plus microscope (Zeiss Microimaging Inc., Thornwood, NY).

LPA and Ki16425 treatment. Eight-week-old WT and *Lpar1*$^{-/-}$ littermates received i.p. injection of 20 mg/kg Ki16425 or were given 1 μg/kg LPA suspended in PBS containing 0.1% BSA by placing LPA into the stomach using a 22-gauge gavage needle once a day for 5 days. Control animals received the same volume of PBS containing 0.1% BSA. Animals were sacrificed 2, 24, or 48 h following BrdU treatment to determine IEC migration as described above.

***In vitro* cell migration and lamellipodium formation.** Cells were seeded on glass coverslips coated with ECM gel (Sigma-Aldrich, St. Louis, MO). Serum-starved confluent monolayer cells were scraped with a pipette tip to create a cell-free region and then incubated with serum-free medium supplemented with LPA for 24 h. Migration into the cell-free area was visualized using a Nikon Eclipse TI microscope (Nikon Instruments Inc., Melville, NY). For detection of lamellipodia, cells were stained for F-actin using phalloidin-Alexa Fluor 568 (Invitrogen). For live cell imaging, time-lapse video microscopy was used. Plates were placed inside a temperature-controlled incubator and mounted on a Carl Zeiss Axiovert microscope equipped with a Zeiss AxioCam MRc5 camera. Images were analyzed using Image J software (NIH, Bethesda, MD).

Cell proliferation. Cells seeded at a density of 2×10^5 cells per well were synchronized by serum starvation for 36 h. For EdU staining, cells were treated with LPA for 24 h, and EdU incorporation into DNA was detected using the Click-iT EdU Alexa Fluor imaging kit according to the manufacturer's instructions (Invitrogen). For the cell proliferation assay, cells were treated with LPA once a day for up to 3 days and the number of cells was counted daily using a hemocytometer.

Confocal immunofluorescence microscopy. Migrating cells were washed twice with cold PBS, fixed in 4% paraformaldehyde in PBS for 10 min at room temperature, permeabilized in 0.2% Triton X-100 in PBS for 5 min, and blocked in PBS containing 5% normal goat serum for 30 min at room temperature. Cells were then stained with primary antibody overnight at 4°C. Following three washes, for 10 min each, with PBS, the cells were incubated with Alexa Fluor 488-conjugated donkey anti-mouse IgG or Alexa Fluor 555-conjugated goat anti-rabbit IgG (Invitrogen) for 1 h at room temperature. After 3 10-min washes with PBS, cells were mounted with ProLong Gold antifade reagent (Invitrogen) and observed under a Zeiss LSM510 laser confocal microscope.

RT-PCR. RT-PCR and real-time RT-PCR were performed using AmpliTaq Gold PCR master mix (Invitrogen) and iQ SYBR green Supermix (Bio-Rad, Hercules, CA), respectively, as previously described (5). The following primer pairs were used: cyclin D1, 5′-TGCGTGCAGAAGGAGATTGT-3′ and 5′-CTTCTTCAAGGGCTCCAGGG-3′; Cdk4, 5′-TACAGCTACCAGATGGCCCT-3′ and 5′-CAACTGGTCGGCTTCAGAGT-3′; cyclin E1, 5′-CTCCCACAACATCCAGACCC-3′ and 5′-TCATTCTGTCTCCTGCTCGC-3′; Cdk2, 5′-TACCCAGTACTGCCATCCGA-3′ and 5′-GACACGGTGAGAATGGCAGA-3′; and c-Myc, 5′-GGTTTGCCTCTTCTCCACAG-3′ and 5′-TCCTGTACCTCGTCCGATTC-3′. Primer sequences for LPA receptors were previously reported (5).

Flow cytometry. Cells seeded at a density of 2×10^5 cells per well were synchronized by serum starvation for 36 h and then incubated with serum-free medium supplemented with LPA for 24 h. Cells were collected with Accutase (Invitrogen), washed in cold phosphate-buffered saline, and fixed in cold 70% ethanol. To determine cell cycle distribution, cells were resuspended in a solution containing 0.1 mg/ml propidium iodide, 0.3% Triton X-100, and 1 mg/ml RNase A and analyzed using BD FACSDiva (BD Biosciences) and FlowJo software (Tree Star, Ashland, OR).

Rac1 and RhoA activity assays. RhoA activity was determined as described previously (18). Activation of Rac1 was determined using a Rac1 activation assay kit (Cytoskeleton Inc., Denver, CO).

Western immunoblot and immunoprecipitation. Western blotting and immunoprecipitation were performed as previously described (6). Isolation of nuclear proteins for the detection of Gαq and PLC-β1 was done using the NE-PER reagents kit (Thermo Fisher Scientific, Rockford, IL). Coimmunoprecipitation of LPA_1, G proteins, PLC-β2, and Rac1 was performed using the catch and release system (EMD Millipore, Billerica, MA) according to the manufacturer's instructions.

Colonoscopy in live mice. Eight-week-old WT and *Lpar1*$^{-/-}$ littermates were anesthetized by intraperitoneal injection of a ketamine (100 mg/kg)-xylazine (10 mg/kg) solution. To create intestinal mucosal wounds and monitor wound closure, we used a high-resolution colonoscopy system equipped with biopsy forceps (19, 20). This system consisted of a miniature rigid endoscope (1.9-mm outer diameter) (Hopkins II telescope; Karl Storz GmbH & Co. KG, Tuttlingen, Germany), a xenon light source, a triple-chip high-resolution charge-coupled device (CCD) camera, and an operating sheath with 3Fr. Endoscopic procedures were viewed with high-resolution (1,024- by 768-pixel) images on a flat-panel color monitor. Wound size averaged ~1 mm^2, which is equivalent to removal of ~250 to 300 crypts (21). In each experiment, 10 to 15 lesions from 5 to 6 mice per group were examined (22).

Induction of colitis. Experimental colitis was induced by adding dextran sodium sulfate (DSS; molecular mass, 36 to 50 kDa; MP Biomedicals, Santa Ana, CA) to the drinking water at a concentration of 3% (wt/vol) for 7 days. At day 7, mice were divided into 2 groups, with one group receiving 20 mg/kg Ki16425 every day by i.p. injection and the other receiving PBS and being allowed to recover by drinking water for an additional 6 days. The disease activities (diarrhea, occult blood, and weight loss) were quantified as we described previously (23). Each parameter was assigned scores of stool consistency and bleeding, adapted from Cooper et al. (23, 24). Mice were sacrificed on either day 7 or day 13.

Histology. Histological parameters were determined in a blinded fashion by two experienced gastrointestinal pathologists as previously described (25) with some modification. Briefly, H&E sections of Swiss roll mounts of entire mouse colons were assessed for the percentage of the mucosa containing ulceration or crypt epithelial injury/damage/active inflammation comprising at least one-third of the thickness of the mucosa by using Aperio's ImageScope viewer (Aperio, Vista, CA). The ulceration and injury/damage values were added and reported as a histologic damage index.

Statistical analysis. Data are expressed as means ± standard errors of the means (SEM). Statistical significance was determined by one-way analysis of variance (ANOVA). *P* values of <0.05 were considered significant.

RESULTS

LPA_1 coupling with Gαq regulates intestinal epithelial cell migration and proliferation. YAMC cells are nontransformed mouse colonic epithelial cells that have previously been used to study signaling involved in IEC viability and migration (15, 16). YAMC cells express LPA_1, LPA_2, and LPA_4 but lack LPA_3 and LPA_5 (see Fig. S1A in the supplemental material). In agreement with a previous report (4), LPA induced migration (5% ± 2.5%, versus 95% ± 3.0% with LPA) (Fig. 1A; see also Fig. S1B in the supplemental material) and proliferation ($2.0 \times 10^5 \pm 0.7 \times 10^5$ cells versus $7.5 \times 10^5 \pm 0.8 \times 10^5$ cells with LPA on day 2) (Fig. 1B) of YAMC cells. However, these LPA-induced effects were markedly decreased by inhibition of LPA_1 by Ki16425, an inhibitor of LPA_1 and LPA_3, as well as stable knockdown of LPA_1, which decreased LPA_1 expression by 69%. Conversely, stable expression of LPA_1 enhanced migration of YAMC cells (Fig. 1C; see also Fig. S1C in the supplemental material) whereas overexpression of LPA_2 had no effect. Similarly, knockdown of LPA_1 inhibited LPA-induced migration and proliferation of other IEC cell lines, MSIE and IEC-6, both of which express LPA_1 (see Fig. S1D in the supplemental material). Lamellipodial protrusions play an important role in forward cell movement. Prominent F-actin-rich lamellipodial protrusions were observed following LPA treatment, which was ablated by knockdown of LPA_1 (Fig. 1D; see also Fig. S1E in the supplemental material). Similarly to cell migration, proliferation of YAMC cells was augmented by overexpression of LPA_1 but not by LPA_2 overexpression (Fig. 1E). Together, these results show that LPA facilitates IEC migration and proliferation via LPA_1.

LPA receptors interact with heterotrimeric G proteins to regulate signaling pathways. To identify G proteins coupled with LPA_1, we coimmunoprecipitated LPA_1 and G proteins. Figure 2A shows that Gαq and Gα13 coimmunoprecipitated with LPA_1 and, importantly, that the interaction with LPA_1 was enhanced by LPA. Despite the frequent involvement of Gαi in GPCR-mediated cell migration, Gαi did not interact with LPA_1 and PTX did not affect LPA_1-dependent epithelial cell migration, ruling out the role of Gαi (Fig. 2B, left panel). Inhibition of Gαq by the Gαq C-terminal minigene blocked LPA-induced cell migration (96% ± 4.0%, versus 57% ± 2.5% with mini-Gαq), but surprisingly, the Gα13 minigene did not show any effect. The specific influence of Gαq in mediating cell migration was confirmed by overexpression of Gα proteins, which showed that Gαq, but not Gαi and Gα13, markedly potentiated cell migration (Fig. 2B, right panel). Consistently, the Gαq minigene abrogated LPA-induced formation of lamellipodia (Fig. 2C).

To determine which G protein is involved in cell proliferation, we compared the effects of inhibiting Gα13, Gαq, and Gαi. Expression of antagonist Gαq minigene abrogated LPA-induced cell proliferation ($9.3 \times 10^5 \pm 0.7 \times 10^5$ cells versus $4.0 \pm 1.0 \times 10^5$ cells with mini-Gαq on day 2), whereas Gα13 minigene and PTX had a marginal effect (Fig. 2D). Hence, both proliferative and migratory effects of LPA_1 are specifically coupled to Gαq protein, and despite its interaction with LPA_1, Gα13 was not involved.

LPA_1-dependent cell migration and proliferation are mediated by distinct PLC-β subtypes. PLC-β is a major effector of Gαq (10). Functional involvement of PLC-β in LPA-induced cell migration was demonstrated by the PLC inhibitor U73122 that abrogated cell migration (Fig. 3A). To identify the specific PLC-β subtypes, YAMC cells transfected with Flag-tagged PLC-β1 to -4

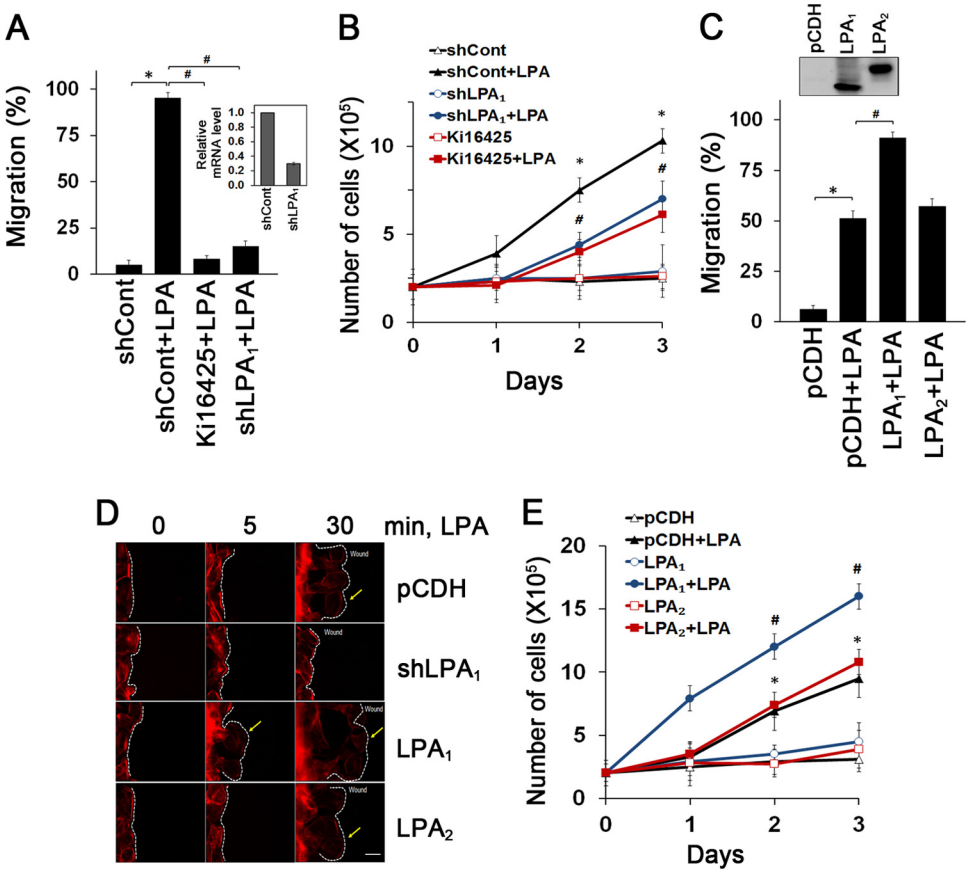

FIG 1 Enhanced intestinal epithelial cell migration and proliferation are LPA_1 dependent. (A) Migration of YAMC cells into the nude area at 24 h of 1 μM LPA treatment is shown. Cells were pretreated with 10 μM Ki16425 or transfected with $shLPA_1$ prior to LPA treatment. The extent of wound closure was quantified. Full recovery of the wound was considered 100%. *, $P < 0.001$; #, $P < 0.001$. $n = 3$. BSA (0.1%) was used as a control. The inset shows LPA_1 knockdown efficacy determined by real-time RT-PCR ($shLPA_1$; 69% decrease). (B) LPA-induced cell proliferation was determined by counting cells for up to 3 days. Cells were pretreated with Ki16425 or transfected with $shLPA_1$ as indicated. *, $P < 0.01$ versus shCont; #, $P < 0.01$ versus shCont plus LPA. Error bars represent the means ± SEM from three independent experiments involving triplicates. (C) The extent of migration at 12 h of LPA treatment was determined. *, $P < 0.01$; #, $P < 0.01$. $n = 4$. The inset shows overexpression of LPA_1 and LPA_2 in YAMC cells. (D) Lamellipodial extrusions in cells transfected with pCDH, $shLPA_1$, LPA_1, or LPA_2 are shown. Cells were fixed and labeled with phalloidin-Alexa Fluor 568 to identify the leading edge of lamellipodia (arrows). Dashed lines indicate the leading edges. $n = 3$. Bar, 20 μm. (E) Numbers of proliferating cells transfected with LPA_1 or LPA_2 were determined. *, $P < 0.01$ versus pCDH; #, $P < 0.01$ compared with pCDH plus LPA. $n = 3$.

were treated with LPA. We found that LPA induced coimmunoprecipitation of Gαq with PLC-β1 and PLC-β2 but not with PLC-β3 and PLC-β4 (Fig. 3B). To determine which of PLC-β1 and PLC-β2 is involved in LPA_1-mediated cellular outcomes, cells with knockdown of either PLC-β1 or PLC-β2 were studied. Knockdown of PLC-β2, but not PLC-β1, significantly abrogated LPA-induced cell migration (94% ± 3.5%, versus 45% ± 7.0% with shPLC-β2) (Fig. 3C). We then asked whether Gαq and PLC-β2 are spatially organized during directional cell migration. LPA induced colocalization of PLC-β2 and Gαq at the leading edge (Fig. 3D). However, PLC-β1 and PLC-β3 were not detected at the lamellipodial protrusion (Fig. 3D, bottom panel).

We next determined whether PLC-β is also involved in cell proliferation. Unlike the effect on cell migration, knockdown of PLC-β1 significantly attenuated LPA-mediated proliferation of YAMC cells ($7.1 \times 10^5 \pm 0.5 \times 10^5$ cells versus $4.6 \times 10^5 \pm 0.5 \times 10^5$ cells with shPLC-β1 on day 2) while PLC-β2 knockdown showed no effect (Fig. 3E). These data show that Gαq-coupled LPA_1 regulates cell proliferation and migration by activating two distinct PLC-βs, PLC-β1 and PLC-β2, respectively.

LPA_1 regulates cell cycle progression to mediate cell proliferation. To further understand the role of PLC-β1 in cell proliferation, we first determined the effects of LPA on cell cycle progression. Flow cytometric analyses showed that LPA induced the G_1-to-S-phase transition (Fig. 4A). This transition was blocked by silencing of LPA_1 or PLC-β1 expression but not by PLC-β2 knockdown. These data suggest a specific role of PLC-β1 in regulating LPA_1-mediated transition from G_1 to S phase. Cell cycle progression is regulated by protein complexes composed of cyclins and cyclin-dependent kinases (CDKs) (26). Hence, we determined whether LPA regulates the expression of cyclins and CDK2. LPA induced expression of cyclin D1 and Cdk4 but not cyclin E1 or Cdk2, consistent with the cell cycle analysis that LPA promotes the G_1-to-S transition (Fig. 4B) (27). Knockdown of either LPA_1 or PLC-β1 but not PLC-β2 decreased LPA-induced cyclin D1 and Cdk4 expression (Fig. 4C). Moreover, Gαq minigene, but not Gα13 minigene or PTX, inhibited the induction of cyclin D1 and Cdk4 (see Fig. S2 in the supplemental material). These results were further confirmed by Western blots showing that LPA-induced cyclin D1 and Cdk4 expression is LPA_1, PLC-β1, and Gαq depen-

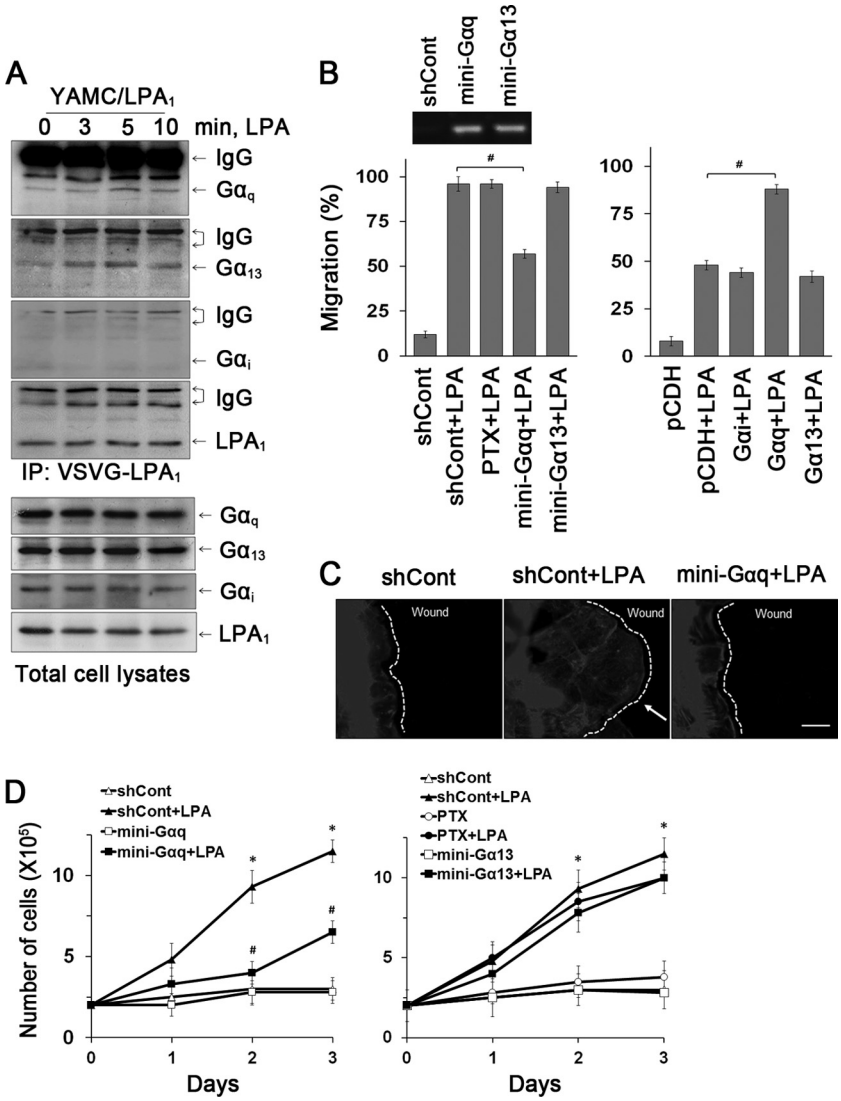

FIG 2 Gαq is essential for LPA_1-mediated cell migration and proliferation. (A) The interaction of Gα subunits with LPA_1 in YAMC/LPA_1 was determined by coimmunoprecipitation of LPA_1 and Gα subunits (top four panels). Expression of Gα subtypes in cell lysates is shown in the bottom panels. $n = 3$. (B) The role of Gα subtypes in cell migration was determined. YAMC cells pretreated with PTX or transfected with Gα minigenes were treated with LPA for 24 h (left panel). The inset shows the presence of Gα minigenes in transfected cells. The right panel shows the effect of Gα subunit overexpression on migration during 12 h of LPA treatment. #, $P < 0.01$. $n = 3$. Full recovery of the wound was considered 100%. #, $P < 0.01$. $n = 3$. (C) Lamellipodial extrusions labeled with phalloidin-Alexa Fluor 568 are shown. Dashed lines indicate the leading edges. $n = 3$. Bar, 20 μm. (D) Effects of inhibition of G proteins on proliferation are determined. (Left) Inhibition of Gαq. (Right) Inhibition of Gαi or Gα13. $n = 3$. *, $P < 0.01$ compared with shCont; #, $P < 0.01$ versus shCont plus LPA. $n = 3$.

dent (Fig. 4D). Together, these results suggest that LPA_1 mediates cell cycle transition from G_1 to S phase via Gαq- and PLC-β1-dependent pathways.

LPA_1 regulates nuclear translocation of Gαq to mediate cell proliferation. To gain insight into how PLC-β1 might take part in cell proliferation, we determined its cellular localization in cells treated with LPA or vehicle. Figure 5A shows that PLC-β1 (red) is highly expressed in the nucleus while Gαq (green) is in both cytoplasm and the nucleus. Importantly, LPA increased the immunofluorescence signal of Gαq and PLC-β1 in the nuclei. A quantitative analysis of colocalization of either Gαq or PLC-β1 with nuclear acid staining by TO-PRO showed a significant increase in the colocalization coefficient induced by LPA. Consistent with the confocal data, a Western blot of nuclear protein fraction (Fig. 5B) shows that LPA elevated Gαq expression in the nucleus without altering total cellular expression. PLC-β1 expression in the nuclei was enhanced by LPA, but increased total PLC-β1 expression was evident. Importantly, knockdown of LPA_1 attenuated the increase in Gαq and PLC-β1 expression. These results indicate that LPA_1 regulates cell proliferation by inducing Gαq and PLC-β1 interaction in the nucleus.

LPA_1 requires the interaction between PLC-β2 and Rac1 to mediate cell migration. LPA activates the RhoA family of GTPase (28, 29). To assess the involvement of Rac1 or RhoA, YAMC cells were treated with Rac1 inhibitor (NSC23766) or ROCK inhibitor (Y-27632), respectively. NSC23766, but not Y-27632, abolished LPA-induced cell migration, suggesting the participation of Rac1 (97% ± 4.0%, versus 32% ± 2.5% with NSC23766) (Fig. 6A).

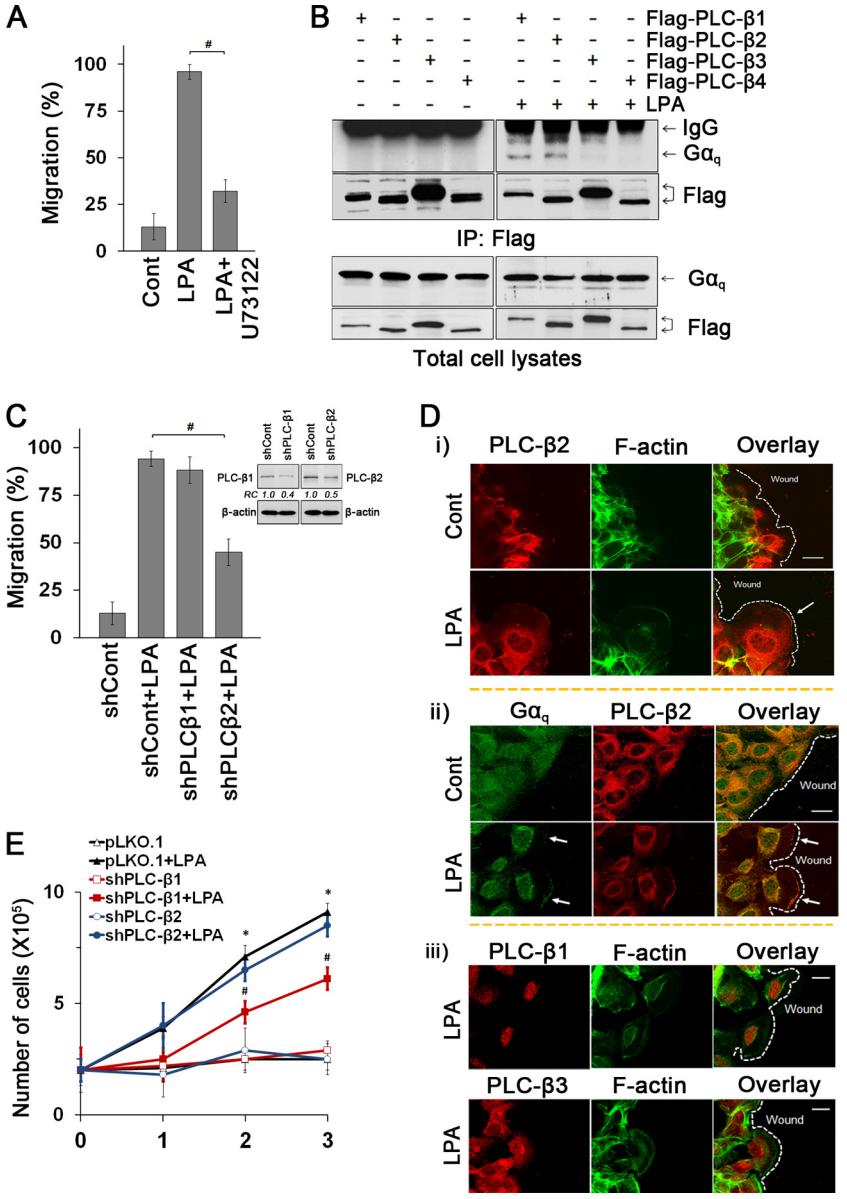

FIG 3 LPA_1 mediates cell migration and proliferation via distinct PLC-β subtypes. (A) The PLC inhibitor U73122 blocked LPA-induced migration. #, $P < 0.001$. $n = 3$. (B) Gαq coimmunoprecipitated with Flag-PLC-β1 and Flag-PLC-β2. Expression of Flag-PLC-βs and Gαq in cell lysates is shown in bottom panels. (C) Effects of PLC-β1 and PLC-β2 knockdown on cell migration were compared. #, $P < 0.01$. $n = 3$. The inset shows the efficacy of PLC-β1 or PLC-β2 knockdown as determined by Western blotting: shPLC-β1, 61% decrease; shPLC-β2, 51% decrease. (D) Cellular distributions of PLC-β2 and F-actin (i), PLC-β2 and Gαq (ii), and PLC-β1 and PLC-β3 (iii) in cells treated with LPA or carrier for 30 min are shown. Arrows indicate lamellipodia. Dashed lines show the leading edges. $n = 3$. Bars, 20 μm. (E) Effects of PLC-β knockdown on proliferation were determined. *, $P < 0.01$ versus shCont; #, $P < 0.01$ versus shCont plus LPA. $n = 3$.

Figure 6B shows that LPA-induced Rac1 activity is determined by pulldown of GTP-bound Rac1. Rac1 activation was augmented by overexpression of LPA_1, whereas knockdown of LPA_1 ablated the effect. Because RhoA is often involved in cell migration, we determined RhoA activation in YAMC cells. LPA stimulated RhoA activity, but surprisingly, RhoA activation was abolished by LPA_1 overexpression (see Fig. S3A in the supplemental material). In contrast, LPA_2 overexpression potentiated RhoA activity, indicating contrasting effects of LPA_1 and LPA_2 on RhoA in YAMC cells. Fig. S3B in the supplemental material shows that the Gαq minigene abrogated LPA-induced activation of Rac1, suggesting that coupling of Gαq with LPA_1 is necessary for Rac1 activity. To affirm the functional importance of Rac1, YAMC cells were transfected with Rac1, constitutively active Rac1G12V, or dominant-negative Rac1T17N. Fig. S3C in the supplemental material shows that Rac1G12V induced migration of YAMC cells even in the absence of LPA. In contrast, LPA failed to stimulate cell migration in the presence of Rac1T17N. These data show that LPA_1-induced cell migration requires active Rac1.

Although PLC-β signaling is known to regulate Rac1 via protein kinase C-dependent mechanisms, evidence shows that PLC-β activity is regulated by the Ras GTPases (30–33). Hence, we next

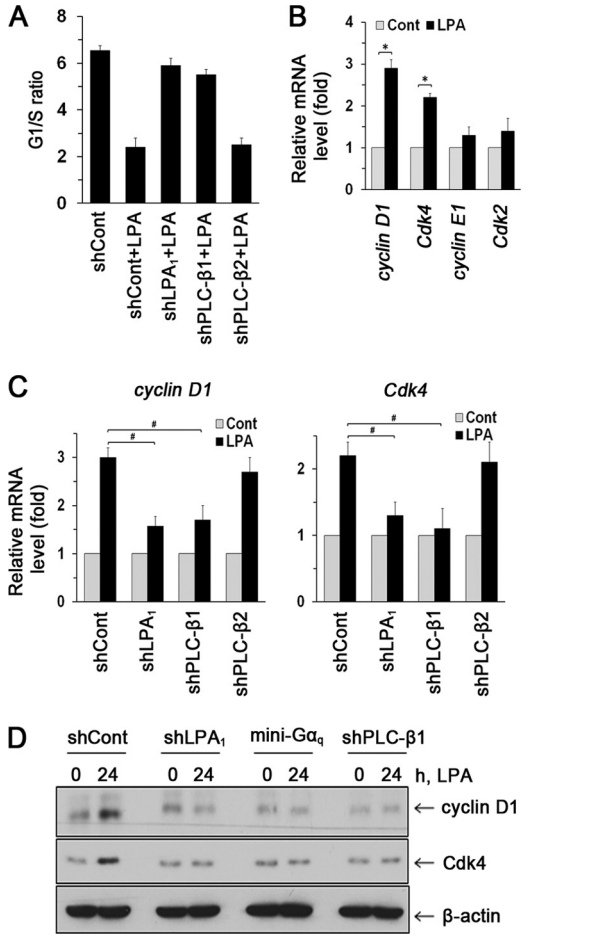

FIG 4 LPA_1 regulates cell cycle progression. (A) G_1/S ratios in cells treated with LPA are shown. $n = 3$. (B) Expression levels of cyclin D1, Cdk4, cyclin E1, and Cdk2 were determined by real-time RT-PCR. $n = 3$. *, $P < 0.01$. (C) Expression levels of cyclin D1 and Cdk4 mRNA are shown. $n = 3$. #, $P < 0.01$. (D) Expression levels of cyclin D1 and Cdk4 were determined by Western blotting. Representative blots from three independent experiments are shown.

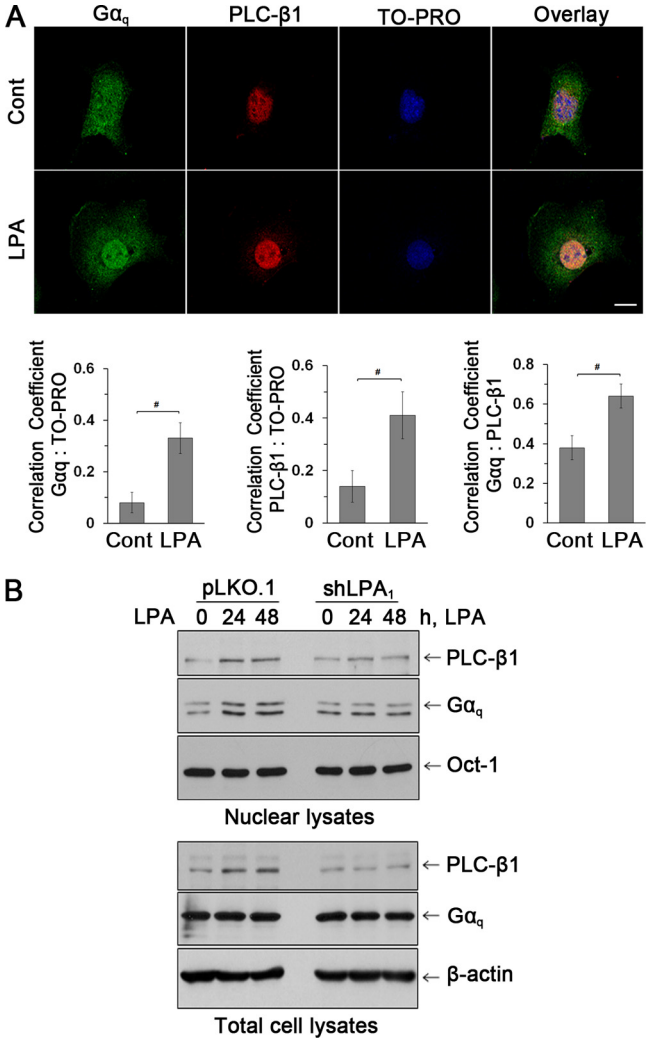

FIG 5 LPA increased the nuclear abundance of Gαq and PLC-β1. (A) Expression of Gαq (green) and PLC-β1 (red) in the nuclei of YAMC cells was assessed by confocal immunofluorescence microscopy. TO-PRO iodide was used for nuclear counterstaining (blue). $n = 3$. Bars, 20 μm. Graphs represent Pearson's coefficient of colocalization of Gαq and TO-PRO (left), PLC-β1 and TO-PRO (middle), and Gαq and PLC-β1 (right) from 10 independent fields of cells. #, $P < 0.05$. (B) Western blot of Gαq and PLC-β1 in nuclear and total cell extracts. The transcription factor Oct-1 was used as a loading control for nuclear proteins. $n = 3$.

determined whether PLC-β2 is important for LPA-mediated Rac1 activation. First, we determined Rac1 activation in cells expressing Flag-PLC-β. Figure 6C shows that LPA activated Rac1 only in cells expressing PLC-β2. Moreover, the interaction between GTP-Rac1 and PLC-β2 was LPA_1 dependent (Fig. 6D). Importantly, knockdown of PLC-β2 markedly decreased LPA-induced activation of Rac1, demonstrating that PLC-β2 regulates Rac1 activity (Fig. 6E). Analogous to Gαq and PLC-β2 (Fig. 3D), LPA induced colocalization of Rac1 with PLC-β2 at the leading edge of cells (see Fig. S3D in the supplemental material). Consistently, LPA enhanced the endogenous interaction between Rac1 and PLC-β2 (see Fig. S3E in the supplemental material). Together, these results suggest that LPA_1 uniquely regulates epithelial cell migration by controlling the PLC-β2-Rac1 interaction at the lamellipodial leading edge.

***Lpar1*$^{-/-}$ mice exhibit impaired intestinal epithelial cell migration and proliferation.** Our previous study showed that LPA_1 is the most abundant LPA receptor in mouse intestinal tract based on the abundance of LPA_1 mRNA (5, 9). Despite its abundance, the specific physiological role of LPA_1 in the intestine remains elusive. To determine the physiological role of LPA_1 and the significance of our *in vitro* findings, we analyzed intestinal epithelial homeostasis in *Lpar1*$^{-/-}$ mice. We found that numbers of proliferating IECs identified by EdU labeling were significantly decreased in *Lpar1*$^{-/-}$ crypts compared to WT crypts (Fig. 7A). This difference in IEC proliferation in *Lpar1*$^{-/-}$ mice was further confirmed by Ki67 staining (see Fig. S4A in the supplemental material). On the other hand, the absence of LPA_1 did not alter the level of apoptosis in the small intestine and colon (see Fig. S4B in the supplemental material).

To assess IEC migration, BrdU pulse-chase experiments were performed. Figure 7B shows that in WT intestine, BrdU-positive IECs migrated upwards such that by 48 h these cells reached the middle of the villi. This was more pronounced in the colon, where

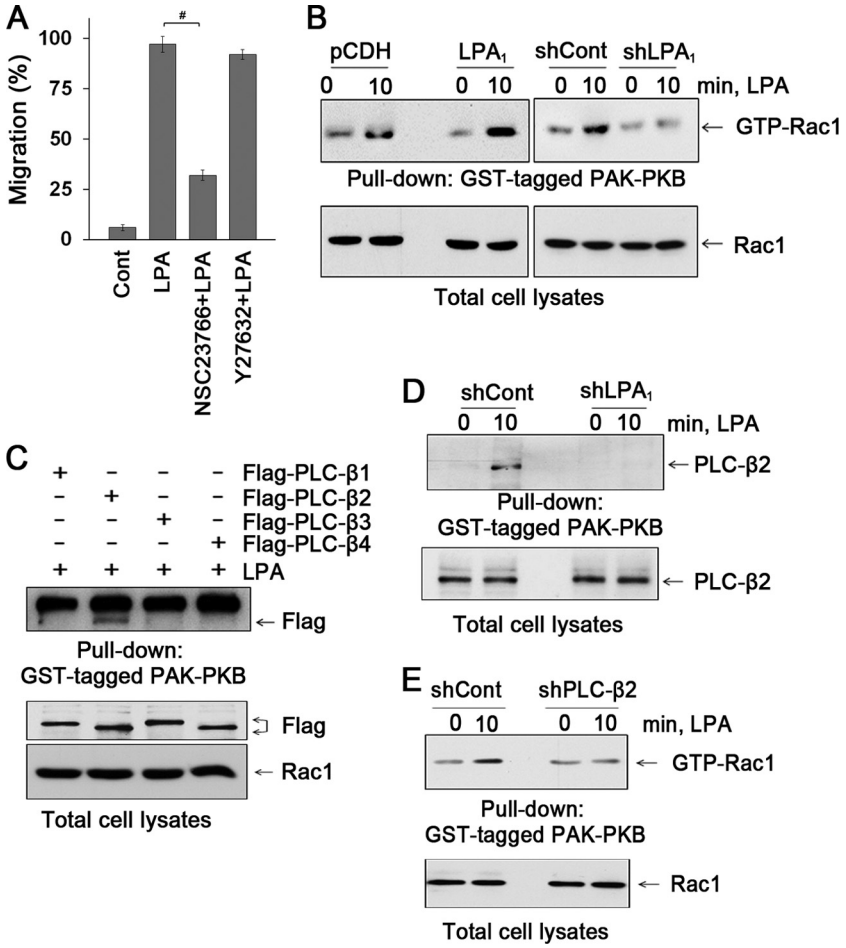

FIG 6 LPA induces the interaction between PLC-β2 and Rac1. (A) Effects of NSC23766 and Y-27632 on cell migration were determined by wound closure assays. $n = 3$. #, $P < 0.01$. (B) The effect of LPA on activation of Rac1 was determined. Cells were treated with LPA for 10 min, and activated Rac1 was isolated with GST-PAK-PBD domain. $n = 3$. (C) The interaction of PLC-β isozymes with activated Rac1 was determined. Flag-PLC-βs were copurified with activated Rac1 in GST-PAK-PBD pulldown assays. The bottom panels show PLC-βs and Rac1 in cell lysates. $n = 4$. (D) Knockdown of LPA_1 attenuated the interaction between PLC-β2 and activated Rac1. $n = 3$. (E) Knockdown of PLC-β2 attenuated activation of Rac1 by LPA. $n = 3$.

cells reached the luminal surface by 48 h. In comparison, BrdU-labeled cells in *Lpar1*$^{-/-}$ intestine and colon were clustered largely at the crypt base at 24 h and migrated at significantly reduced rates. Together, the above-mentioned data show novel findings that the absence of LPA_1 results in impaired IEC proliferation and subsequent upward movement of enterocytes from crypts to villi. Interestingly, the heights of villi along the entire length of the small intestine were shorter in *Lpar1*$^{-/-}$ mice than in wild-type (WT) animals (see Fig. S5A in the supplemental material). The shortening of villi was not accompanied by a change in villous width or spacing of villi. However, unlike the small intestine, colonic crypt depth was not altered and the crypt structures remained similar between the two strains. Heterozygosity of LPA_1 did not result in morphological changes (see Fig. S5B in the supplemental material). Likewise, *Lpar2*$^{-/-}$ mice did not show any change in intestinal mucosal morphology (see Fig. S5C in the supplemental material). These data provide the first evidence that a loss of LPA_1 results in a significant morphological defect in the intestine.

To ensure that the defects observed in *Lpar1*$^{-/-}$ intestine were a direct consequence of loss of LPA_1 function, we tested the effect of the LPA_1 inhibitor Ki16425 on WT mice. Mice were given 20 mg/kg Ki16425 according to previous studies (34, 35). We anticipated that 5 days is a minimum duration for the inhibitor to take an effect based on the life span of epithelial cells in mouse intestine. Ki16425 treatment decreased cell migration and proliferation in the small intestine and colon (Fig. 7C). In comparison, oral administration of LPA to WT mice enhanced migration of BrdU-labeled cells compared with control-treated mice. Although the change in numbers of proliferating cells in the intestine was not readily discernible, a decrease in BrdU-labeled cells in the colon was apparent. Unlike WT mice, LPA did not alter the rate of cell migration or proliferating IEC numbers in *Lpar1*$^{-/-}$ mice (Fig. 7D), suggesting that the novel effects are mediated mainly through LPA_1.

Because LPA promotes proliferation of IECs *in vitro* by regulating Gαq and PLC-β1 expression, we examined Gαq and PLC-β1 expression in mice treated with LPA. Gαq and PLC-β1 were located mainly in the proliferating crypt compartment of the intestinal tract, and importantly, LPA significantly increased expression of Gαq (Fig. 8A) and PLC-β1 (Fig. 8B) in the nuclei of WT crypt epithelial cells. However, LPA failed to stimulate Gαq and PLC-β1 expression in *Lpar1*$^{-/-}$ mice, confirming the specific role of LPA_1 in modulating Gαq and PLC-β1 expression. To-

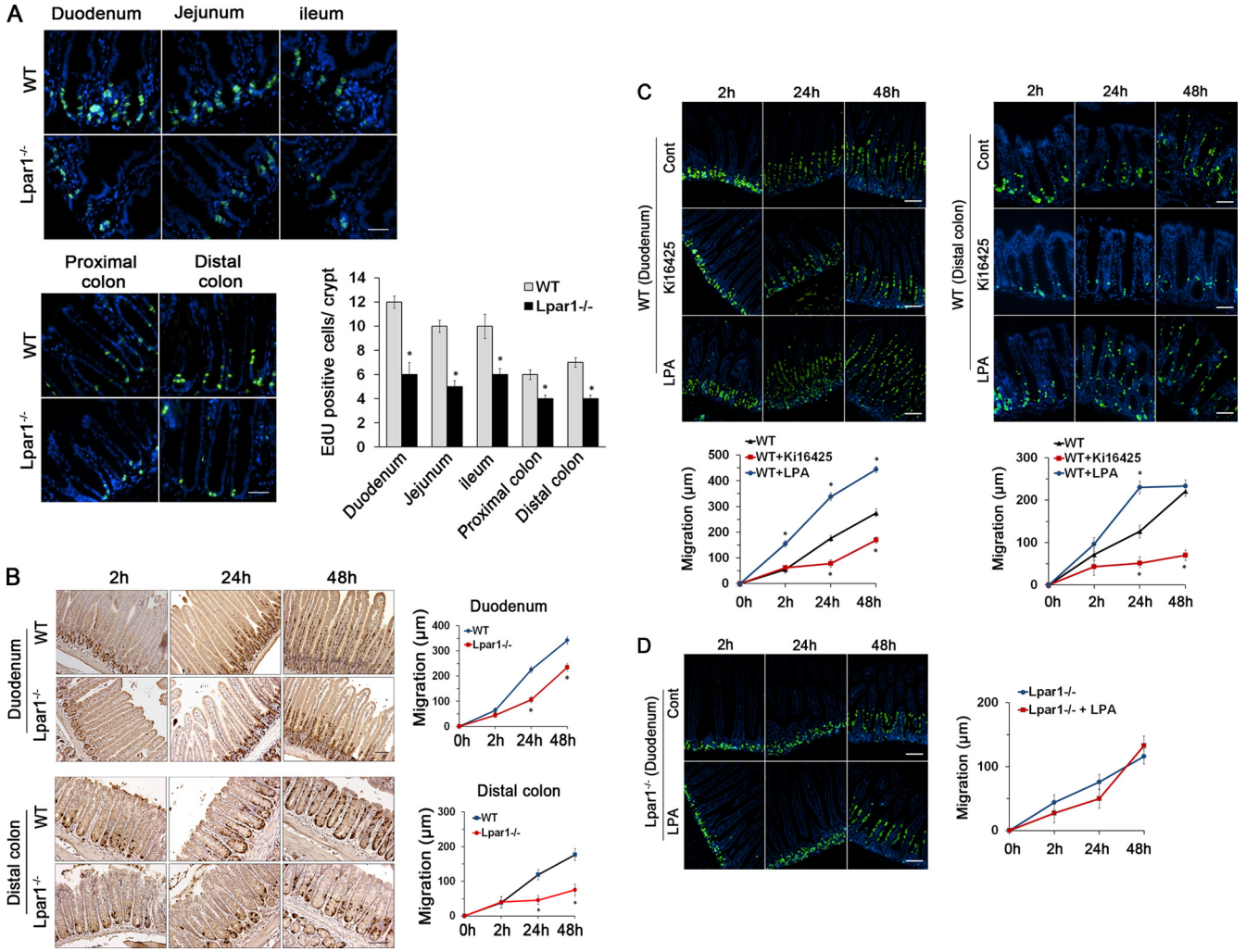

FIG 7 *Lpar1*$^{-/-}$ mice display decreased numbers of proliferating cells and impeded cell migration. (A) Proliferating IECs of WT and *Lpar1*$^{-/-}$ mice were identified by EdU staining (green). DAPI (4′,6-diamidino-2-phenylindole) was used for nuclear counterstaining (blue). The mean numbers of EdU-labeled cells per crypt are shown in the bar graph. $n = 8$ per group. Bars, 100 μm. *, $P < 0.05$. (B) Migration of proliferating IECs along the crypt-villus axis was determined by BrdU pulse-chase for indicated times in duodenum (top) and in distal colon (bottom). The extent of cell migration was quantified by measuring the distance between the crypt base and the highest labeled cell along the crypt-villus axis. Bars, 100 μm. $n = 8$. *, $P < 0.01$ versus the WT. (C) Migration of IECs was determined in mice given an i.p. injection of Ki16425 or LPA orally for 5 days. Time-dependent migration of BrdU-positive cells (green) in WT duodenum (left) and distal colon (right) are shown. $n = 6$. DAPI was used for nuclear counterstaining (blue). Bars, 50 μm. *, $P < 0.01$ versus the WT. (D) IEC migration in *Lpar1*$^{-/-}$ duodenum treated with LPA or not is shown. Bars, 50 μm. $n = 8$.

gether, these data demonstrate that the LPA-LPA$_1$ signaling axis promotes cell proliferation by regulating Gαq and PLC-β1 expression in proliferating intestinal epithelial cells. Based on these findings, we propose a model that LPA$_1$ regulates IEC homeostasis, encompassing proliferation and migration, via two distinct PLC-βs (Fig. 8C).

LPA$_1$ requires epithelial mucosal wound repair. Having demonstrated the defects of *Lpar1*$^{-/-}$ mice in IEC homeostasis, we sought to determine the roles of LPA and LPA$_1$ in efficient mucosal wound closure and barrier recovery. Defined mechanical colonic mucosal wounds were generated using a mouse endoscopy-guided biopsy forceps (Fig. 9A and B). The rates of wound closure in WT and *Lpar1*$^{-/-}$ mice were determined by quantifying wound resealing from the images captured at the wounded sites. To assess the role of LPA in epithelial wound closure, LPA was delivered orally once a day. LPA enhanced mucosal wound repair in WT mice compared with that in control-treated mice. In contrast, *Lpar1*$^{-/-}$ mice showed a significant delay in wound repair and LPA did not promote wound repair in *Lpar1*$^{-/-}$ mice. To further demonstrate the role of LPA$_1$ in colonic mucosal wound repair, WT mice were given DSS for 7 days to induce acute colitis. At day 7, one half of the mice were given Ki16425 daily for the next 6 days while the other half received an equal volume of PBS as a control. Analysis of disease activity index (24) revealed that the cohort that received Ki16425 had delayed-recovery DSS-induced colitis compared to the control group (Fig. 9C). Histologic examination showed that epithelial ulceration and crypt damage from DSS-induced colitis were almost completely restored in the control cohort. In contrast, significant mucosal epithelial damage and inflammation were observed in Ki16425-treated mice (Fig. 9D and E). Together, these results demonstrate the unique role of LPA$_1$ in mediating epithelial mucosal wound repair.

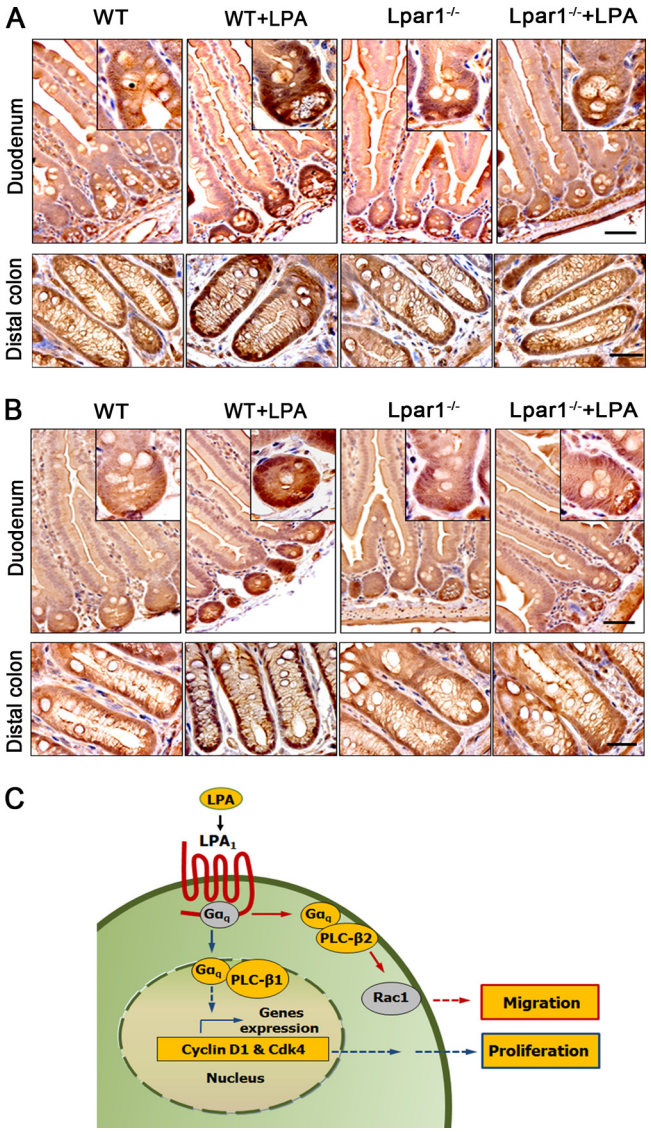

FIG 8 LPA stimulates the expression of Gαq and PLC-β1 in the proliferating crypt compartment of the intestinal tract. Intestinal sections of WT and *Lpar1*$^{-/-}$ mice treated with LPA were stained with anti-Gαq (A) or anti-PLC-β1 (B) antibody. $n = 5$. Bars, 50 μm. (C) A model of LPA_1-dependent effects on IECs is shown.

DISCUSSION

Cells often express more than one PLC-β, and a body of evidence suggests that despite the similar structure and regulatory mode shared by all subtypes of PLC-β, each PLC-β supports distinct functions (10). How cells selectively regulate multiple PLC-β isozymes is not clearly understood. A key finding of our study is that LPA_1 regulates two different cellular outcomes through two distinct PLC-β isozymes, PLC-β1 and PLC-β2. As depicted in Fig. 8C, LPA acts through Gαq, leading to activation of PLC-β2 and Rac1 at the plasma membrane to induce cell migration. Gαq, at the same time, diffuses into the nucleus, where it couples with PLC-β1 to mediate cell cycle progression, resulting in increased cell proliferation. Hence, these findings demonstrate that Gαq activated by the same extracellular cue regulates two closely related PLC-βs via spatial placement within the cell.

PLC-β1 is the major nuclear PLC-β isozyme, but the regulation of nuclear PLC-β1 is not well understood (10). It was shown that insulin-like growth factor 1 (IGF-1) stimulation of 3T3 cells activates Erk1/2, which translocate to the nucleus where they phosphorylate PLC-β1 (36). Avazeri et al. showed that during the resumption of meiosis in mouse oocyte, PLC-β1 translocates to the nucleus, accumulating in the nucleosome (37). In the current study, we observed that LPA increased nuclear expression of Gαq and PLC-β1. G proteins are initially thought to be localized to the plasma membrane, but it is now well accepted that G proteins exist at other cellular locations, including the Golgi apparatus, the endoplasmic reticulum, and even the nucleus (38). Although LPA induced nuclear abundance of Gαq without an effect on total Gαq expression levels, an increase in cellular PLC-β1 expression was noted. Hence, this suggests that LPA increases PLC-β1 nuclear abundance in part by stimulation of PLC-β1 expression. It was shown that GPCRs, including LPA_1, are present on the nuclear envelope (39, 40). Hence, it is plausible that LPA stimulates nuclear LPA_1 that activates Gαq and PLC-β1 to produce inositol 1,4,5-triphosphate in the nucleus. However, this raises another question of how extracellular LPA can cross the plasma membrane to reach the nuclear envelope. In addition to nuclear targeting of Gαq and PLC-β1 by LPA, PLC-β1 plays a key role in regulation of the cell cycle in number of cell types (41, 42). We provide compelling evidence that LPA_1 is required for the Gαq-mediated PLC-β1 pathway in facilitating the cell cycle transition from G_0/G_1 to S phase. Although PLC-β1 couples cell cycle machinery (41, 42), the unique association of PLC-β1 with LPA_1-mediated cell cycle progression has not been reported. Intriguingly, LPA acting on LPA_1 induced cyclin D1 and its catalytic partner Cdk4, which are known to play important roles in the G_1/S checkpoint of the cell cycle in a PLC-β1-dependent manner, indicating that PLC-β1 is a relevant target to link LPA_1-elicited selective proliferative responses. In support of these findings, our *in vivo* results revealed that LPA increased Gαq and PLC-β1 expression in the proliferating crypt compartment of the intestinal tract in mice. However, a similar change was absent in *Lpar1*$^{-/-}$ mice, affirming the role of LPA_1 in Gαq and PLC-β1 activation. The lack of effect on Gαq and PLC-β1 expression in *Lpar1*$^{-/-}$ mice correlates with the decreased numbers of proliferating IECs observed in *Lpar1*$^{-/-}$ mice. These findings hence identify LPA_1 as a major signaling regulator of Gαq and PLC-β1 in IEC proliferation.

Migrating cells undergo a striking transition in cell shape that is regulated by cytoskeletal reorganization orchestrated by the Rho GTPases RhoA, Rac, and Cdc42 (43). LPA activated both Rac1 and RhoA in YAMC cells. However, unlike Rac1, RhoA activation was inhibited by overexpression of LPA_1. We suggest that RhoA activation is mediated by LPA_2 since YAMC cells express LPA_2, which potentiated RhoA activation when overexpressed. In B103 neuroblast cells, LPA_1 promotes cell migration by activating Rac through a Gi-mediated pathway that involves phosphoinositide 3-kinase and Tiam1 (29). Interestingly, Tiam1, which promotes Rac activity and cell migration, suppresses RhoA activity. Hence, our results are consistent with the notion that LPA_1 promotes cell migration by coordinating Gq-mediated activation of Rac1 and inhibition of RhoA.

PLC-β interacts with Gαq and Rac1 through its C-terminal region and PH domain, respectively (30, 44). We found that activated Rac1 specifically binds to PLC-β2 and that the interaction was selectively activated by LPA acting on LPA_1. Moreover, LPA

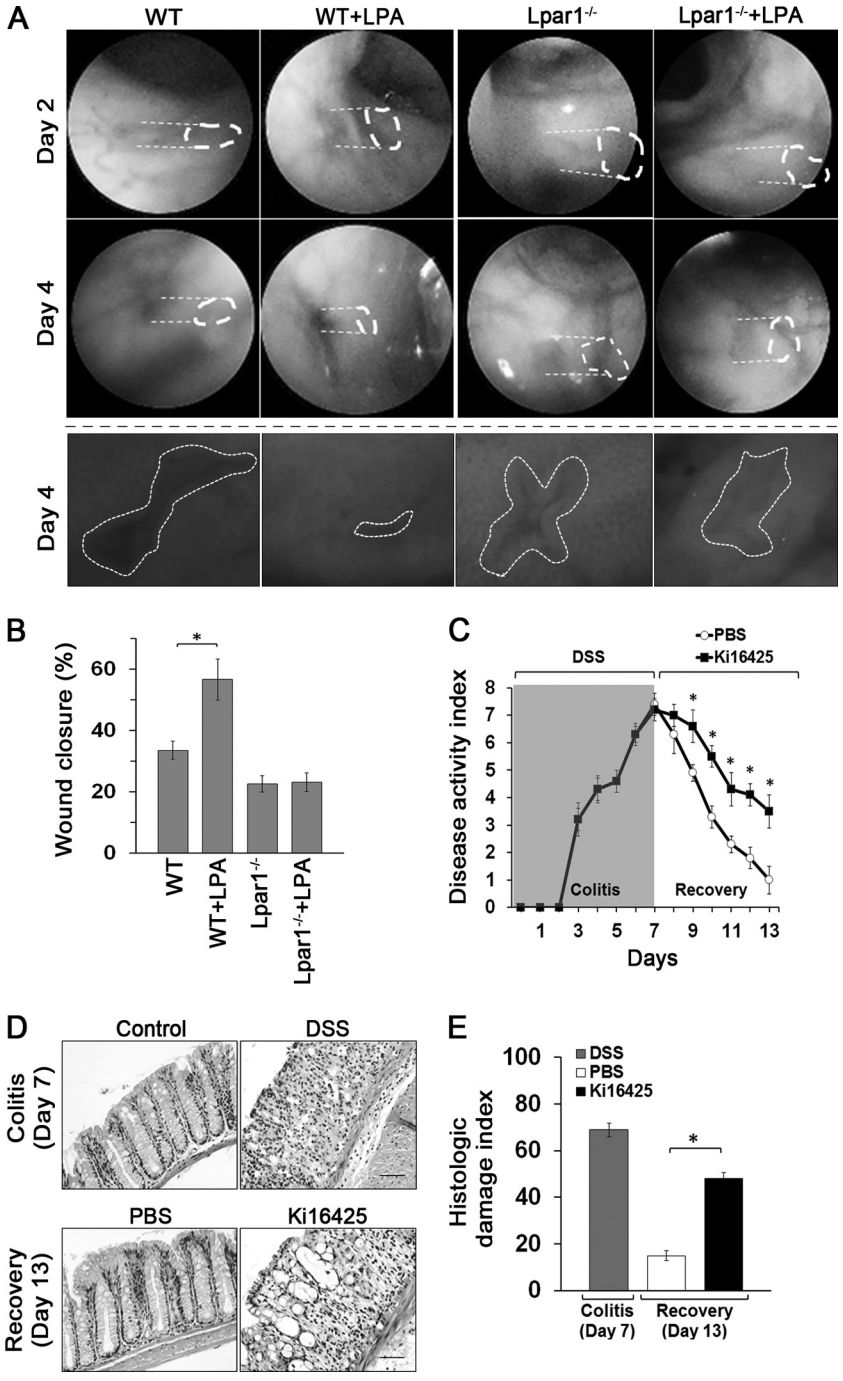

FIG 9 LPA_1 requires epithelial mucosal wound repair. (A) Colonic mucosal wounds were induced in WT and *Lpar1*$^{-/-}$ mice by mouse colonoscopy biopsy. Mice were given LPA or carrier by gavage for 4 days. Representative colonoscopy images of colonic mucosal wound healing at day 2 and day 4 after biopsy-induced injury are shown. Close-up images of colonic mucosa wounds at day 4 are shown below. (B) Quantification of wound repair (means ± SEM) relative to original wound size is shown in the graph below. $n = 6$ per group. *, $P < 0.01$. (C) WT mice were subjected to DSS for 7 days to induce acute colitis. At day 7, mice were divided into 2 groups ($n = 8$), with one group receiving Ki16425 (20 mg/kg) every day by i.p. injection and the other receiving PBS. Clinical disease activity indexes of mice are shown. $n = 8$. *, $P < 0.01$ versus PBS. (D) Representative colonic tissues stained with H&E are shown. $n = 8$. Bars, 100 μm. (E) Histologic damage index scores from whole mouse colons are shown. *, $P < 0.01$ versus PBS. $n = 8$.

induced colocalization of Rac1 and PLC-β2 at the plasma membrane of lamellipodia. This colocalization with Rac1 at lamellipodia was unique to PLC-β2, as neither PLC-β1 nor PLC-β3 was detected at the leading edge. Thus, these results suggest that LPA enhances dynamic membrane targeting of activated Rac1 and PLC-β2 to make a close cooperation with cell migration machinery and that LPA_1 uniquely controls these processes.

Our *in vivo* study identifies LPA_1 as a key regulator of epithelial cell proliferation and migration in the intestine. Loss of LPA_1 impeded mucosal restitution of wounded areas in the colon, demon-

strating clinical importance of LPA_1. To our knowledge, this is the first study demonstrating a relationship between the LPA_1 receptor and enterocyte proliferation and migration in the intestine. In addition to a loss of the LPA_1 gene, pharmacological inhibition of LPA_1 resulted in decreased epithelial cell proliferation and migration. Ki16425 has a short half-life *in vivo*, and so it was not expected to work as well as genetic deletion. However, the effects induced by Ki16425 suggest that brief LPA_1 antagonism is sufficient to produce a detectable difference in the intestinal tract.

Genetic deletion of LPA_1 in mice results in perinatal lethality, craniofacial dysmorphism, and abnormal bone development (16, 45). However, *Lpar1*$^{-/-}$ mice do not appear to show gross differences in the intestinal functions and do not exhibit apparent signs of inflammation or diarrhea. Interestingly, however, we found that the intestinal villous height was reduced in *Lpar1*$^{-/-}$ mice. This difference might have been caused by decreased proliferation in the crypt that results in a loss of force pushing the cells upward. However, given the profound effect of LPA_1 on IEC migration, we suggest that defective epithelial cell proliferation and migration together contribute to the decreased villous height. Whether LPA_1 is expressed in intestinal stem cells or transit-amplifying cells has yet to be determined, but LPA_1 expression has been observed in the embryonic brain (46, 47). Another plausible cause of decreased villous height in *Lpar1*$^{-/-}$ mice is altered food consumption. However, it was reported that food consumption of *Lpar1*$^{-/-}$ mice does not differ from that of WT mice (48), and we have not observed a significant difference in daily food consumption between WT and *Lpar1*$^{-/-}$ mice housed at Emory (S.-J. Lee and C. C. Yun, unpublished data).

In keeping with LPA_1 stimulating IEC migration and proliferation, our *in vivo* study shows that LPA facilitated wound repair in the colon and loss of LPA_1 reduced the wound-healing capacity of LPA. Congruently, an earlier study has shown that LPA ameliorates epithelial damage in chemical-induced colitis in rats, although receptor specificity was not able to be determined from this study (4). In addition, LPA_1 is the most abundant LPA receptor in the intestine (7). Therefore, the absence of LPA_1 reduced healing of mechanical biopsy-induced injury, and consistently, inhibition of LPA_1 markedly impeded recovery from DSS-induced colitis. Certain foods are rich in LPA (49), and hence, our study presents the possibility that LPA-rich foods may affect the homeostasis of intestinal cell renewal and enhance healing of epithelial damage. Recently, LPA_1 has been linked to pulmonary and renal fibrosis (50, 51), and clinical trials to test the efficacy of LPA_1 inhibitors in treatment of fibrotic diseases are expected to follow. The current findings suggest that careful consideration should be given to the use of LPA_1 inhibitors to treat certain fibrotic disease of patients who might also have gastrointestinal illnesses that can result in adverse events.

In summary, our study shows that LPA_1 regulates cell proliferation and migration through spatial targeting of distinct PLC-β isozymes. In addition, this study has revealed a role of LPA_1 in IEC homeostasis and mucosal repair.

ACKNOWLEDGMENTS

This work was supported by a Senior Research Award from the Crohn's and Colitis Foundation of America, the National Institutions of Health grants DK071597 to C.C.Y., DK055679 to A.N., and MH51699 and NS082092 to J.C., and the German Research Foundation (DFG; NE1834/1-1) to P.-A.N. The microscopy core was supported by grant DK064399.

We declare that no conflict of interest exists.

REFERENCES

1. **Crosnier C, Stamataki D, Lewis J.** 2006. Organizing cell renewal in the intestine: stem cells, signals and combinatorial control. Nat. Rev. Genet. **7**:349–359.
2. **Choi JW, Herr DR, Noguchi K, Yung YC, Lee CW, Mutoh T, Lin ME, Teo ST, Park KE, Mosley AN, Chun J.** 2010. LPA receptors: subtypes and biological actions. Annu. Rev. Pharmacol. Toxicol. **50**:157–186.
3. **Mutoh T, Rivera R, Chun J.** 2012. Insights into the pharmacological relevance of lysophospholipid receptors. Br. J. Pharmacol. **165**:829–844.
4. **Sturm A, Sudermann T, Schulte KM, Goebell H, Dignass AU.** 1999. Modulation of intestinal epithelial wound healing in vitro and in vivo by lysophosphatidic acid. Gastroenterology **117**:368–377.
5. **Lin S, Yeruva S, He P, Singh AK, Zhang H, Chen M, Lamprecht G, de Jonge HR, Tse M, Donowitz M, Hogema BM, Chun J, Seidler U, Yun CC.** 2010. Lysophosphatidic acid stimulates the intestinal brush border Na(+)/H(+) exchanger 3 and fluid absorption via LPA(5) and NHERF2. Gastroenterology **138**:649–658.
6. **Lee SJ, Ritter SL, Zhang H, Shim H, Hall RA, Yun CC.** 2011. MAGI-3 competes with NHERF-2 to negatively regulate LPA2 receptor signaling in colon cancer cells. Gastroenterology **140**:924–934.
7. **Lin S, Lee SJ, Shim H, Chun J, Yun CC.** 2010. The absence of LPA receptor 2 reduces the tumorigenesis by ApcMin mutation in the intestine. Am. J. Physiol. Gastrointest. Liver Physiol. **299**:G1128–G1138.
8. **Li C, Dandridge KS, Di A, Marrs KL, Harris EL, Roy K, Jackson JS, Makarova NV, Fujiwara Y, Farrar PL, Nelson DJ, Tigyi GJ, Naren AP.** 2005. Lysophosphatidic acid inhibits cholera toxin-induced secretory diarrhea through CFTR-dependent protein interactions. J. Exp. Med. **202**:975–986.
9. **Yun CC, Sun H, Wang D, Rusovici R, Castleberry A, Hall RA, Shim H.** 2005. LPA2 receptor mediates mitogenic signals in human colon cancer cells. Am. J. Physiol. Cell Physiol. **289**:C2–C11.
10. **Suh PG, Park JI, Manzoli L, Cocco L, Peak JC, Katan M, Fukami K, Kataoka T, Yun S, Ryu SH.** 2008. Multiple roles of phosphoinositide-specific phospholipase C isozymes. BMB Rep. **41**:415–434.
11. **Ohta H, Sato K, Murata N, Damirin A, Malchinkhuu E, Kon J, Kimura T, Tobo M, Yamazaki Y, Watanabe T, Yagi M, Sato M, Suzuki R, Murooka H, Sakai T, Nishitoba T, Im DS, Nochi H, Tamoto K, Tomura H, Okajima F.** 2003. Ki16425, a subtype-selective antagonist for EDG-family lysophosphatidic acid receptors. Mol. Pharmacol. **64**:994–1005.
12. **Yamada T, Sato K, Komachi M, Malchinkhuu E, Tobo M, Kimura T, Kuwabara A, Yanagita Y, Ikeya T, Tanahashi Y, Ogawa T, Ohwada S, Morishita Y, Ohta H, Im DS, Tamoto K, Tomura H, Okajima F.** 2004. Lysophosphatidic acid (LPA) in malignant ascites stimulates motility of human pancreatic cancer cells through LPA1. J. Biol. Chem. **279**:6595–6605.
13. **Yun CH, Lamprecht G, Forster DV, Sidor A.** 1998. NHE3 kinase A regulatory protein E3KARP binds the epithelial brush border Na+/H+ exchanger NHE3 and the cytoskeletal protein ezrin. J. Biol. Chem. **273**:25856–25863.
14. **Whitehead RH, VanEeden PE, Noble MD, Ataliotis P, Jat PS.** 1993. Establishment of conditionally immortalized epithelial cell lines from both colon and small intestine of adult H-2Kb-tsA58 transgenic mice. Proc. Natl. Acad. Sci. U. S. A. **90**:587–591.
15. **Gilchrist A, Bunemann M, Li A, Hosey MM, Hamm HE.** 1999. A dominant-negative strategy for studying roles of G proteins in vivo. J. Biol. Chem. **274**:6610–6616.
16. **Contos JJ, Fukushima N, Weiner JA, Kaushal D, Chun J.** 2000. Requirement for the lpA1 lysophosphatidic acid receptor gene in normal suckling behavior. Proc. Natl. Acad. Sci. U. S. A. **97**:13384–13389.
17. **He P, Lee SJ, Lin S, Seidler U, Lang F, Fejes-Toth G, Naray-Fejes-Toth A, Yun CC.** 2011. Serum- and glucocorticoid-induced kinase 3 in recycling endosomes mediates acute activation of Na+/H+ exchanger NHE3 by glucocorticoids. Mol. Biol. Cell **22**:3812–3825.
18. **Zhang H, Wang D, Sun H, Hall RA, Yun CC.** 2007. MAGI-3 regulates LPA-induced activation of Erk and RhoA. Cell Signal. **19**:261–268.
19. **Becker C, Fantini MC, Schramm C, Lehr HA, Wirtz S, Nikolaev A, Burg J, Strand S, Kiesslich R, Huber S, Ito H, Nishimoto N, Yoshizaki K, Kishimoto T, Galle PR, Blessing M, Rose-John S, Neurath MF.** 2004. TGF-beta suppresses tumor progression in colon cancer by inhibition of IL-6 trans-signaling. Immunity **21**:491–501.
20. **Becker C, Fantini MC, Wirtz S, Nikolaev A, Kiesslich R, Lehr HA, Galle**

PR, Neurath MF. 2005. In vivo imaging of colitis and colon cancer development in mice using high resolution chromoendoscopy. Gut **54**:950–954.
21. **Manieri NA, Drylewicz MR, Miyoshi H, Stappenbeck TS.** 2012. Igf2bp1 is required for full induction of Ptgs2 mRNA in colonic mesenchymal stem cells in mice. Gastroenterology **143**:110–121.
22. **Pickert G, Neufert C, Leppkes M, Zheng Y, Wittkopf N, Warntjen M, Lehr HA, Hirth S, Weigmann B, Wirtz S, Ouyang W, Neurath MF, Becker C.** 2009. STAT3 links IL-22 signaling in intestinal epithelial cells to mucosal wound healing. J. Exp. Med. **206**:1465–1472.
23. **Lin S, Wang D, Iyer S, Ghaleb AM, Shim H, Yang VW, Chun J, Yun CC.** 2009. The absence of LPA2 attenuates tumor formation in an experimental model of colitis-associated cancer. Gastroenterology **136**:1711–1720.
24. **Cooper HS, Murthy SN, Shah RS, Sedergran DJ.** 1993. Clinicopathologic study of dextran sulfate sodium experimental murine colitis. Lab. Invest. **69**:238–249.
25. **Nava P, Koch S, Laukoetter MG, Lee WY, Kolegraff K, Capaldo CT, Beeman N, Addis C, Gerner-Smidt K, Neumaier I, Skerra A, Li L, Parkos CA, Nusrat A.** 2010. Interferon-gamma regulates intestinal epithelial homeostasis through converging beta-catenin signaling pathways. Immunity **32**:392–402.
26. **Reed SI.** 1992. The role of p34 kinases in the G1 to S-phase transition. Annu. Rev. Cell Biol. **8**:529–561.
27. **Beauchamp RD, Sheng HM, Shao JY, Thompson EA, Ko TC.** 1996. Intestinal cell cycle regulations. Interactions of cyclin D1, Cdk4, and p21Cip1. Ann. Surg. **223**:620–628.
28. **Hama K, Aoki J, Fukaya M, Kishi Y, Sakai T, Suzuki R, Ohta H, Yamori T, Watanabe M, Chun J, Arai H.** 2004. Lysophosphatidic acid and autotaxin stimulate cell motility of neoplastic and non-neoplastic cells through LPA1. J. Biol. Chem. **279**:17634–17639.
29. **Van Leeuwen FN, Olivo C, Grivell S, Giepmans BN, Collard JG, Moolenaar WH.** 2003. Rac activation by lysophosphatidic acid LPA1 receptors through the guanine nucleotide exchange factor Tiam1. J. Biol. Chem. **278**:400–406.
30. **Snyder JT, Singer AU, Wing MR, Harden TK, Sondek J.** 2003. The pleckstrin homology domain of phospholipase C-beta2 as an effector site for Rac. J. Biol. Chem. **278**:21099–21104.
31. **Harden TK, Sondek J.** 2006. Regulation of phospholipase C isozymes by ras superfamily GTPases. Annu. Rev. Pharmacol. Toxicol. **46**:355–379.
32. **Notcovich C, Diez F, Tubio MR, Baldi A, Kazanietz MG, Davio C, Shayo C.** 2010. Histamine acting on H1 receptor promotes inhibition of proliferation via PLC, RAC, and JNK-dependent pathways. Exp. Cell Res. **316**:401–411.
33. **Harmon B, Ratner L.** 2008. Induction of the $G\alpha_q$ signaling cascade by the human immunodeficiency virus envelope is required for virus entry. J. Virol. **82**:9191–9205.
34. **Boucharaba A, Serre CM, Guglielmi J, Bordet JC, Clezardin P, Peyruchaud O.** 2006. The type 1 lysophosphatidic acid receptor is a target for therapy in bone metastases. Proc. Natl. Acad. Sci. U. S. A. **103**:9643–9648.
35. **Ma L, Matsumoto M, Xie W, Inoue M, Ueda H.** 2009. Evidence for lysophosphatidic acid 1 receptor signaling in the early phase of neuropathic pain mechanisms in experiments using Ki-16425, a lysophosphatidic acid 1 receptor antagonist. J. Neurochem. **109**:603–610.
36. **Xu A, Suh PG, Marmy-Conus N, Pearson RB, Seok OY, Cocco L, Gilmour RS.** 2001. Phosphorylation of nuclear phospholipase C beta1 by extracellular signal-regulated kinase mediates the mitogenic action of insulin-like growth factor I. Mol. Cell. Biol. **21**:2981–2990.
37. **Avazeri N, Courtot AM, Pesty A, Duquenne C, Lefevre B.** 2000. Cytoplasmic and nuclear phospholipase C-beta 1 relocation: role in resumption of meiosis in the mouse oocyte. Mol. Biol. Cell **11**:4369–4380.
38. **Willard FS, Crouch MF.** 2000. Nuclear and cytoskeletal translocation and localization of heterotrimeric G-proteins. Immunol. Cell Biol. **78**:387–394.
39. **Waters CM, Saatian B, Moughal NA, Zhao Y, Tigyi G, Natarajan V, Pyne S, Pyne NJ.** 2006. Integrin signalling regulates the nuclear localization and function of the lysophosphatidic acid receptor-1 (LPA1) in mammalian cells. Biochem. J. **398**:55–62.
40. **Gobeil F, Fortier A, Zhu T, Bossolasco M, Leduc M, Grandbois M, Heveker N, Bkaily G, Chemtob S, Barbaz D.** 2006. G-protein-coupled receptors signalling at the cell nucleus: an emerging paradigm. Can. J. Physiol. Pharmacol. **84**:287–297.
41. **O'Carroll SJ, Mitchell MD, Faenza I, Cocco L, Gilmour RS.** 2009. Nuclear PLCbeta1 is required for 3T3-L1 adipocyte differentiation and regulates expression of the cyclin D3-cdk4 complex. Cell Signal. **21**:926–935.
42. **Faenza I, Matteucci A, Manzoli L, Billi AM, Aluigi M, Peruzzi D, Vitale M, Castorina S, Suh PG, Cocco L.** 2000. A role for nuclear phospholipase Cbeta 1 in cell cycle control. J. Biol. Chem. **275**:30520–30524.
43. **Etienne-Manneville S, Hall A.** 2002. Rho GTPases in cell biology. Nature **420**:629–635.
44. **Illenberger D, Schwald F, Pimmer D, Binder W, Maier G, Dietrich A, Gierschik P.** 1998. Stimulation of phospholipase C-beta2 by the Rho GTPases Cdc42Hs and Rac1. EMBO J. **17**:6241–6249.
45. **Gennero I, Laurencin-Dalicieux S, Conte-Auriol F, Briand-Mesange F, Laurencin D, Rue J, Beton N, Malet N, Mus M, Tokumura A, Bourin P, Vico L, Brunel G, Oreffo RO, Chun J, Salles JP.** 2011. Absence of the lysophosphatidic acid receptor LPA1 results in abnormal bone development and decreased bone mass. Bone **49**:395–403.
46. **Estivill-Torrus G, Llebrez-Zayas P, Matas-Rico E, Santin L, Pedraza C, De Diego I, Del Arco I, Fernandez-Llebrez P, Chun J, De Fonseca FR.** 2008. Absence of LPA1 signaling results in defective cortical development. Cereb. Cortex **18**:938–950.
47. **Hecht JH, Weiner JA, Post SR, Chun J.** 1996. Ventricular zone gene-1 (vzg-1) encodes a lysophosphatidic acid receptor expressed in neurogenic regions of the developing cerebral cortex. J. Cell Biol. **135**:1071–1083.
48. **Dusaulcy R, Daviaud D, Pradere JP, Gres S, Valet P, Saulnier-Blache JS.** 2009. Altered food consumption in mice lacking lysophosphatidic acid receptor-1. J. Physiol. Biochem. **65**:345–350.
49. **Tanaka T, Kassai A, Ohmoto M, Morito K, Kashiwada Y, Takaishi Y, Urikura M, Morishige J, Satouchi K, Tokumura A.** 2012. Quantification of phosphatidic acid in foodstuffs using a thin-layer-chromatography-imaging technique. J. Agric. Food Chem. **60**:4156–4161.
50. **Tager AM, LaCamera P, Shea BS, Campanella GS, Selman M, Zhao Z, Polosukhin V, Wain J, Karimi-Shah BA, Kim ND, Hart WK, Pardo A, Blackwell TS, Xu Y, Chun J, Luster AD.** 2008. The lysophosphatidic acid receptor LPA1 links pulmonary fibrosis to lung injury by mediating fibroblast recruitment and vascular leak. Nat. Med. **14**:45–54.
51. **Pradere JP, Klein J, Gres S, Guigne C, Neau E, Valet P, Calise D, Chun J, Bascands JL, Saulnier-Blache JS, Schanstra JP.** 2007. LPA1 receptor activation promotes renal interstitial fibrosis. J. Am. Soc. Nephrol. **18**:3110–3118.